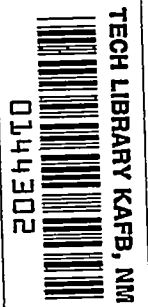


542217

~~CONFIDENTIAL~~

Copy 200  
RM L53J09b

NACA RM L53J09b



~~7~~  
NACA

# RESEARCH MEMORANDUM

7493

APPLICATION OF TRANSONIC AREA RULE TO  
A SHARP-LIPPED DUCTED NACELLE

By Richard E. Walters

Langley Aeronautical Laboratory  
Langley Field, Va. *Wallopsville*

SSR

SR

By

*Langley Aeronautical Laboratory*  
*Langley Field, Va.*

*2 March*

GRADE OR TITLE (PLEASE CHANGE)

*4 April*

~~CONFIDENTIAL~~

This material contains information affecting the National Defense of the United States within the meaning of the espionage laws, Title 18, U.S.C., Secs. 793 and 794, the transmission or revelation of which in any manner to an unauthorized person is prohibited by law.

## NATIONAL ADVISORY COMMITTEE FOR AERONAUTICS

WASHINGTON

January 5, 1954

~~CONFIDENTIAL~~

5148

~~Handwritten scribble~~

1M

NACA RM L53J09b

~~CONFIDENTIAL~~

TECH LIBRARY KAFB, NM



0144302

NATIONAL ADVISORY COMMITTEE FOR AERONAUTICS

RESEARCH MEMORANDUM

APPLICATION OF TRANSONIC AREA RULE TO

A SHARP-LIPPED DUCTED NACELLE

By Richard E. Walters

## SUMMARY

The transonic area rule has been used to determine the equivalent area distributions of two normal-shock, sharp-lipped inlet configurations. Two bodies of revolution having the longitudinal area distributions of the inlet configurations less the areas of the entering free-stream tubes have been flight-tested. The agreement between the measured transonic drag rise from tests of the inlet models and of the bodies of revolution confirmed the method of application of the rule in these cases.

## INTRODUCTION

The transonic area rule of reference 1 states that the zero-lift transonic drag rise of an aircraft configuration is mainly a function of the axial distribution of cross-sectional area normal to the air stream. Previous investigations of the transonic area rule have shown the rule to predict the transonic drag rise of various aircraft configurations as reported in references 2 and 3. Configurations incorporating ducted nacelles pose an additional problem of a method to determine the effective area distribution of the nacelle. One method, as suggested by the author of reference 1, is to represent the area distribution of the nacelle by the area of the external contour less the entering free-stream-tube area. The purpose of this investigation is to investigate the feasibility of such an approach by comparing the transonic drag rise of inlet models with those measured from bodies of equivalent area distribution as determined by the method above.

The results of the drag tests of two normal-shock inlet models (ref. 4) and the corresponding equivalent bodies are presented. These results for the inlet models were obtained from rocket tests of the configurations over a Mach number range of 0.8 to 1.4, corresponding to a Reynolds number range of  $26 \times 10^6$  to  $48 \times 10^6$  based on the body length,

~~CONFIDENTIAL~~~~11/20/54~~

and helium gun tests of 1/4-scale equivalent bodies of revolution between Mach numbers of 0.9 to 1.25 corresponding to a Reynolds number range of  $7 \times 10^6$  to  $11 \times 10^6$  based on body length. The tests were conducted at the Langley Pilotless Aircraft Research Station at Wallops Island, Va.

## SYMBOLS

A	cross-sectional area along longitudinal axis, $\pi r^2$ , in. <sup>2</sup>
A <sub>0</sub>	area of entering free-stream tube, equal to product of mass-flow ratio and inlet area, in. <sup>2</sup>
C <sub>D</sub>	drag coefficient based on maximum frontal area of each model
$\Delta C_D$	drag-rise increment from Mach number of 0.9
L	length, in.
M	Mach number
S	maximum frontal area, in. <sup>2</sup>
S.F.	scale factor, ratio of linear dimensions of equivalent body to corresponding inlet model
X	longitudinal coordinate
r	body radius along longitudinal axis, in.

## CONFIGURATIONS AND TESTS

Drag tests were made on the equivalent bodies of two previously tested inlet configurations, the parabolic inlet models 1 and 3 of reference 4. The inlet model with a mass-flow ratio of 1.0 at Mach number 1.0 is referred to as model 1, the equivalent body as model 1(a), the inlet model with a mass-flow ratio of 0.675 at Mach number 1.0 as model 2, and its corresponding equivalent body as model 2(a).

Figure 1 presents the geometric characteristics of the inlet models of reference 4 and figure 2, the bodies of equivalent area distribution.

Figure 3 shows the external area distributions of the inlet models and the equivalent bodies. The method used to determine the equivalent body was to subtract from the external area distribution of the inlet configuration the area of the entering free-stream tube at Mach number 1,  $A_0$  in the figure. The area  $A_0$  is defined as the product of the mass-flow ratio and the inlet area. The mass-flow ratio for model 1 was 1.00 and for model 2 it was 0.675, both values for a Mach number of 1. The area distributions do not include the fin areas. The fins on the equivalent bodies were scale models of those on the inlet models and were 1/32 inch thick.

The coordinates of the equivalent bodies are presented in table I and in reference 4 for the ducted models. Figure 4 shows the variation of Reynolds number with Mach number for the two sets of models.

Models 1(a) and 2(a) were catapulted by a helium gun to Mach numbers of 1.225 and 1.250, respectively. During the coasting period that followed, the velocity was measured by a CW Doppler radar set. These data were reduced to drag coefficients and Mach numbers by assuming a normal ballistic trajectory.

The total errors for the tests of the equivalent bodies are estimated to be within the following limits:

Mach number, M . . . . .	±0.01
Drag coefficient, $C_D$ . . . . .	±0.01

## RESULTS AND DISCUSSION

Figure 5 presents the drag coefficients, based on maximum model frontal area, for the two sets of models. In figure 6 the drag-rise values are shown. In order to compare the drag-rise values which are absolute quantities, it is necessary to base the drag coefficients on the same reference area. In these cases the reference area was selected as the maximum frontal area of the inlet models. The drag rise was referenced to the drag at a Mach number of 0.9. A comparison of figures 6(a) and 6(b) shows the drag rise to be essentially the same for both models and, consequently, not dependent on mass-flow ratio in these cases.

The results of the tests show that the equivalent bodies determined by this method give the same transonic drag rise as the inlet models.

~~CONFIDENTIAL~~

NACA RM L53J09b

## CONCLUDING REMARKS

A method of applying the transonic area rule concept has been used to determine solid bodies having the equivalent area distributions of two normal-shock, sharp-lipped inlet configurations. The results of the drag tests indicate that the equivalent bodies did have the same transonic drag rise as the corresponding inlet configurations.

Langley Aeronautical Laboratory,  
National Advisory Committee for Aeronautics,  
Langley Field, Va., September 25, 1953.

## REFERENCES

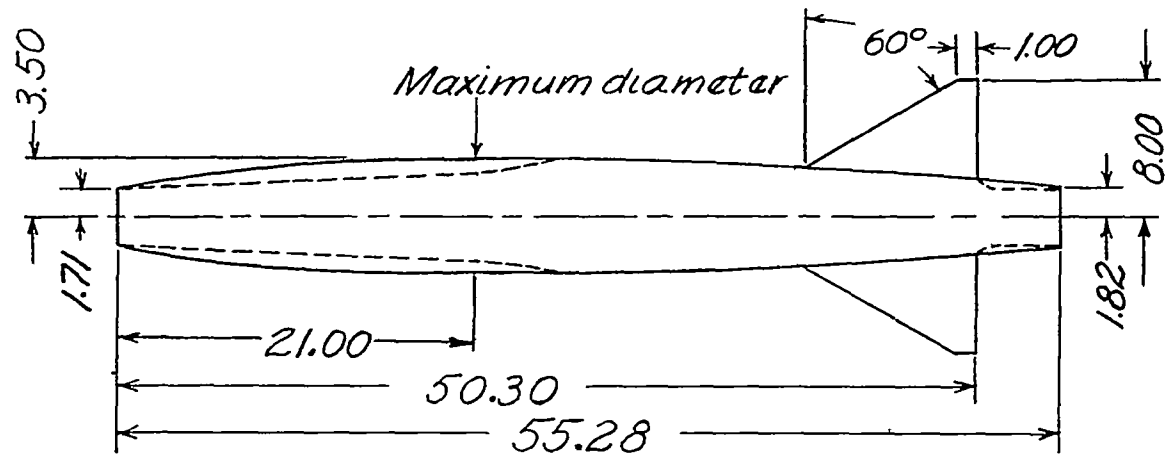
1. Whitcomb, Richard T.: A Study of the Zero-Lift Drag-Rise Characteristics of Wing-Body Combinations Near the Speed of Sound. NACA RM L52H08, 1952.
2. Hopko, Russell N., Piland, Robert O., and Hall, James R.: Drag Measurements at Low Lift of a Four-Nacelle Airplane Configuration Having a Longitudinal Distribution of Cross-Sectional Area Conducive to Low Transonic Drag Rise. NACA RM L53E29, 1953.
3. Hall, James Rudyard: Comparison of Free-Flight Measurements of the Zero-Lift Drag Rise of Six Airplane Configurations and Their Equivalent Bodies of Revolution at Transonic Speeds. NACA RM L53J21a, 1953.
4. Sears, R. I., Merlet, C. F., and Putland, L. W.: Flight Determination of Drag of Normal-Shock Nose Inlets With Various Cowling Profiles at Mach Numbers From 0.9 to 1.5. NACA RM L53I25a, 1953.

~~CONFIDENTIAL~~

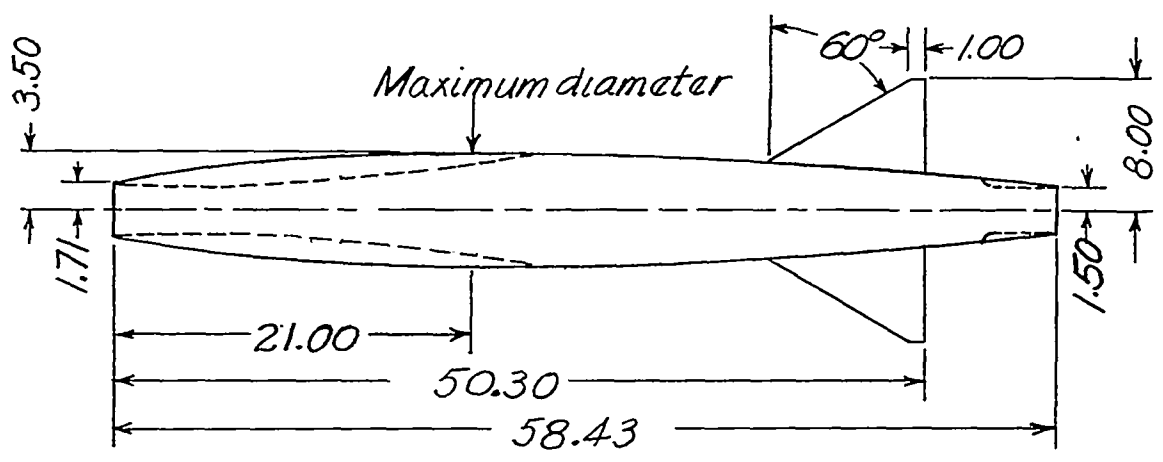
TABLE I.- COORDINATES OF EQUIVALENT BODIES

Model 1(a)		Model 2(a)	
X/L	r/L	X/L	r/L
0	0	0	0.0167
.018	.014	.017	.0214
.036	.020	.034	.0253
.054	.025	.051	.0287
.072	.029	.068	.0318
.109	.035	.103	.0372
.145	.041	.154	.0438
.181	.045	.188	.0473
.217	.048	.222	.0500
.253	.051	.274	.0530
.289	.053	.308	.0541
.326	.054	.342	.0547
.362	.055	.359	.0548
.380	.055	.407	.0547
.431	.055	.503	.0530
.532	.053	.567	.0507
.599	.051	.631	.0480
.667	.048	.727	.0422
.768	.041	.822	.0342
.870	.031	.886	.0279
.937	.024	.928	.0227
.971	.019	.947	.0198
.981	.016	.971	.0157
1.000	.011	1.000	.0050

~~CONFIDENTIAL~~~~CONFIDENTIAL~~



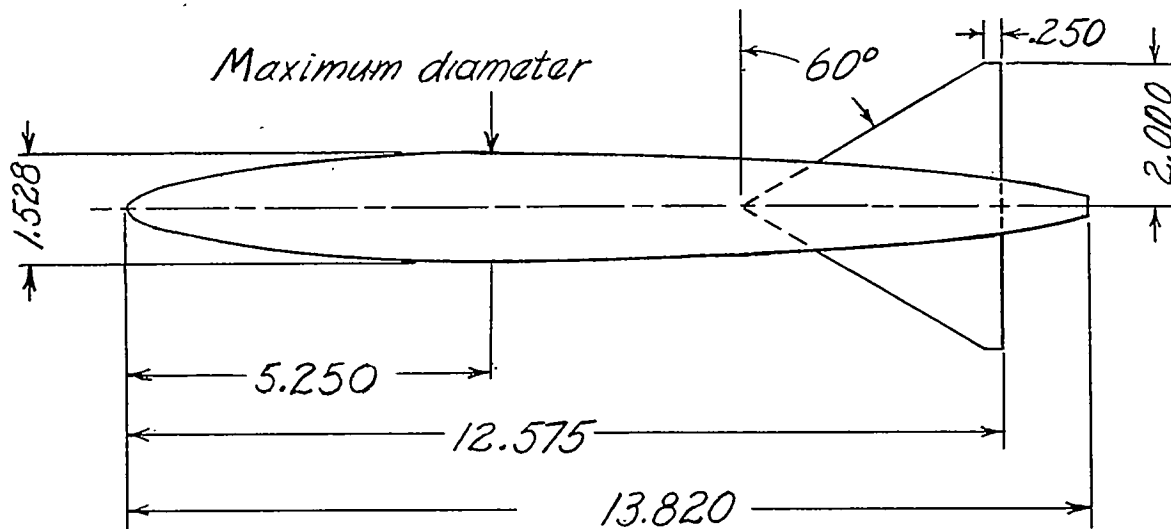
(a) Model 1.



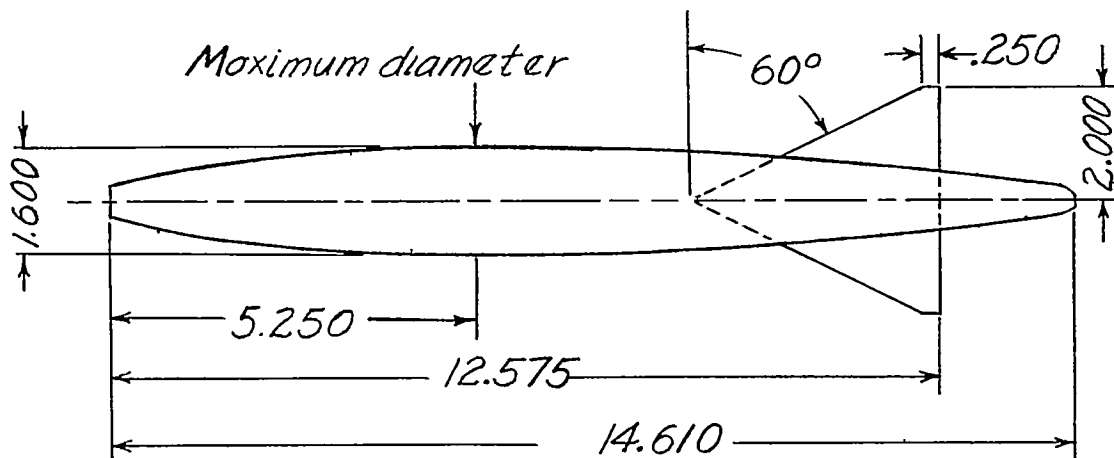
(b) Model 2.

Figure 1.- Inlet models. All dimensions are in inches.

~~CONFIDENTIAL~~



(a) General arrangement of model 1(a).

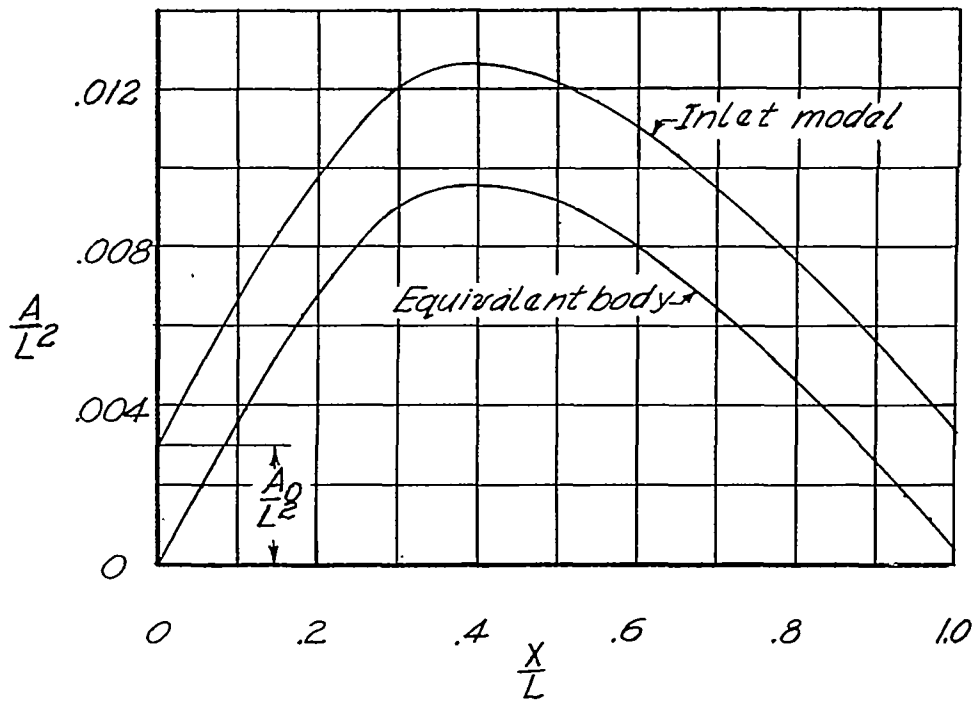


(b) General arrangement of model 2(a).

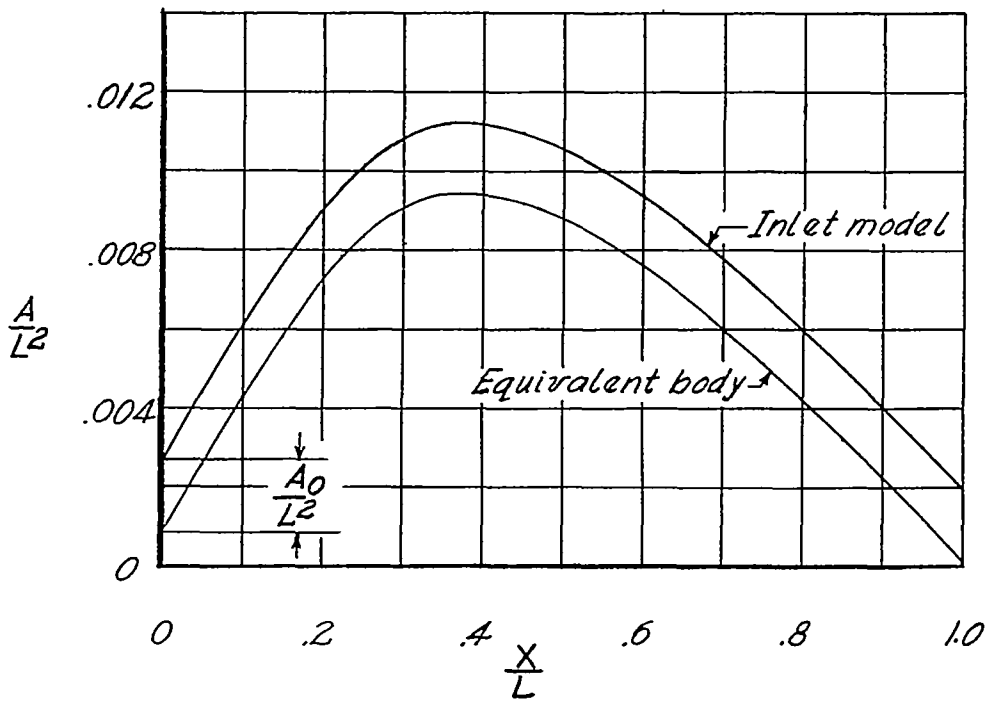
Figure 2.- Bodies of equivalent area distribution. All dimensions are in inches.

~~CONFIDENTIAL~~



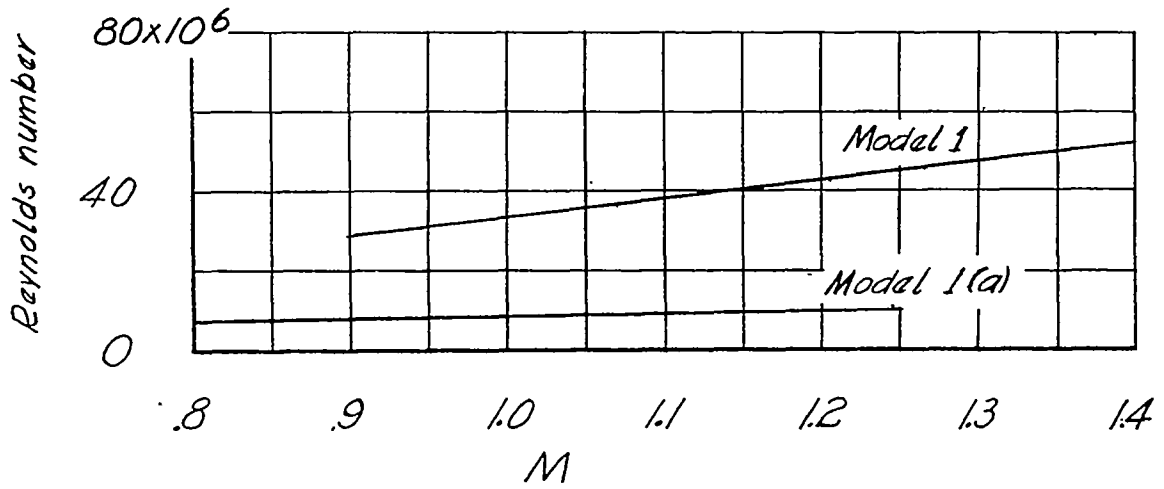


(a) Model (1) and equivalentent body 1(a).

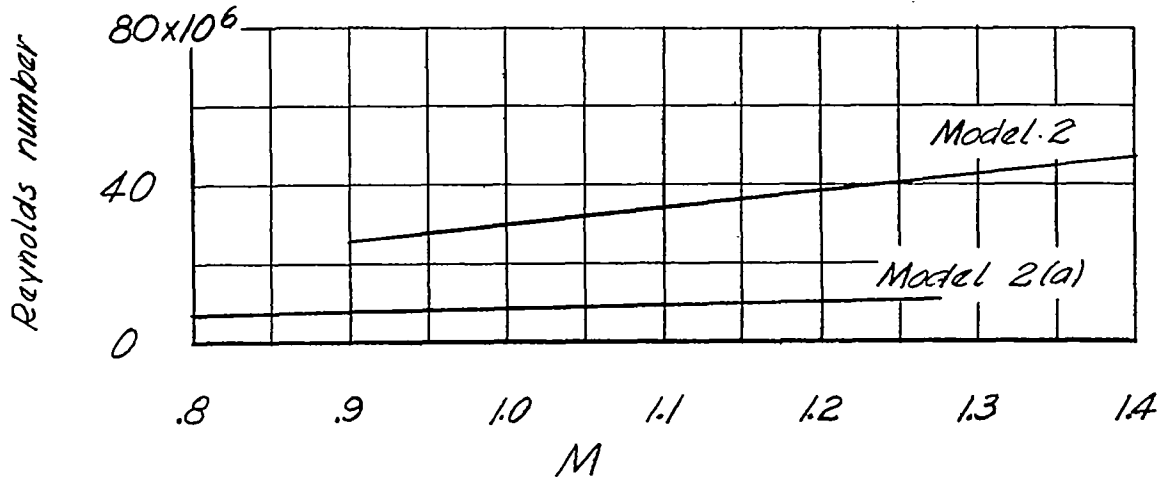


(b) Model (2) and equivalentent body 2(a).

Figure 3.- Longitudinal area distribution of models investigated.

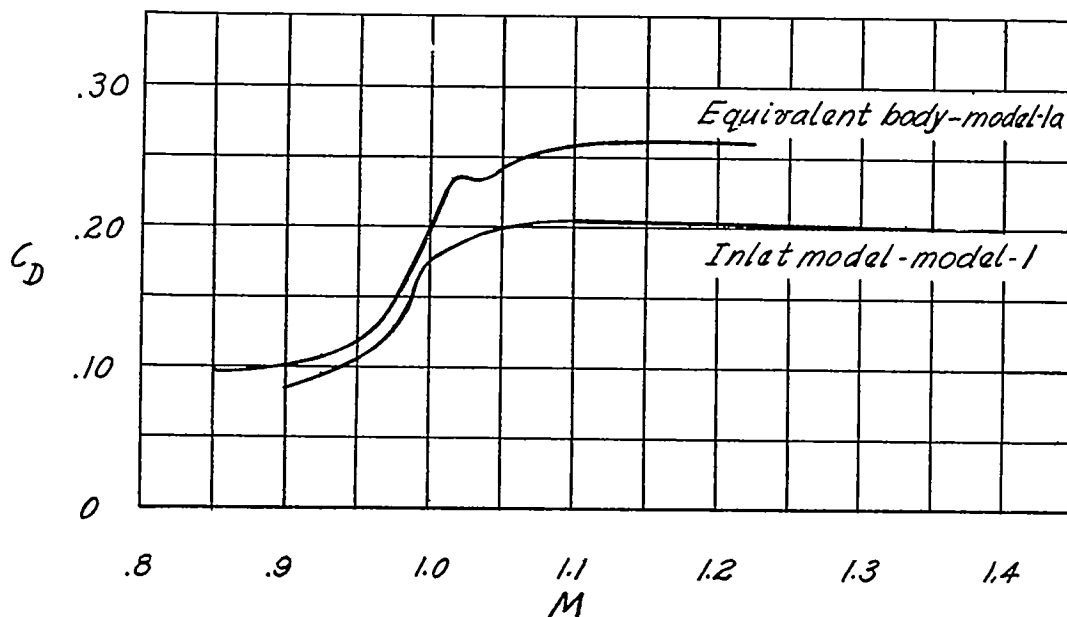


(a) Model 1 and model 1(a).

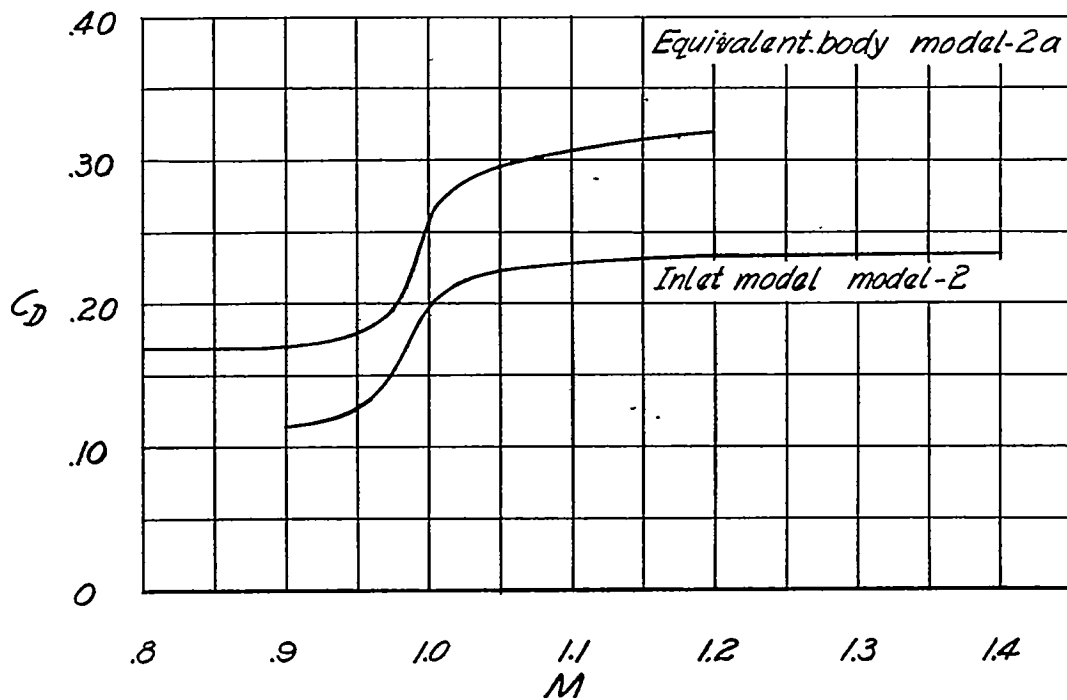


(b) Model 2 and model 2(a).

Figure 4.- Variation of Reynolds number, based on body length, with Mach number.

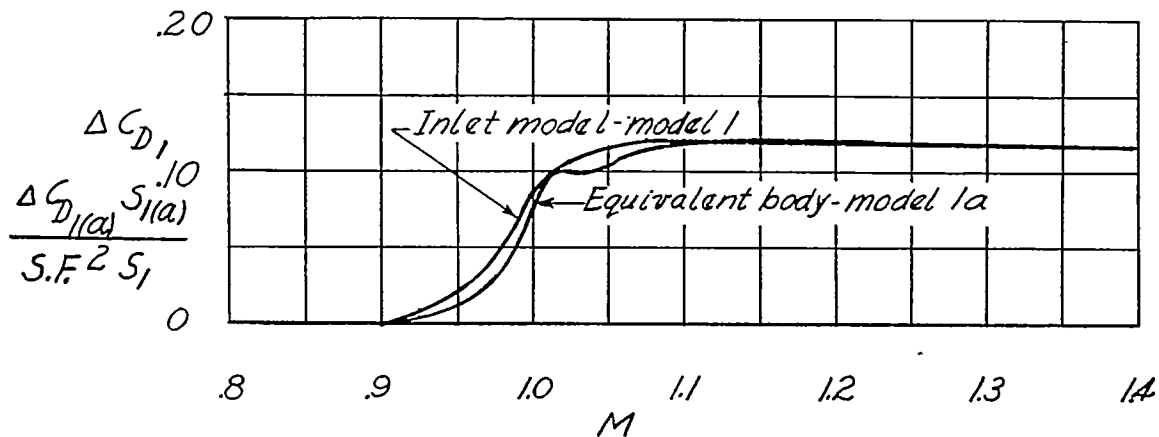


(a) Models 1 and 1(a);  $S_1 = 38.5$  sq in.;  $S_{1(a)} = 1.83$  sq in.

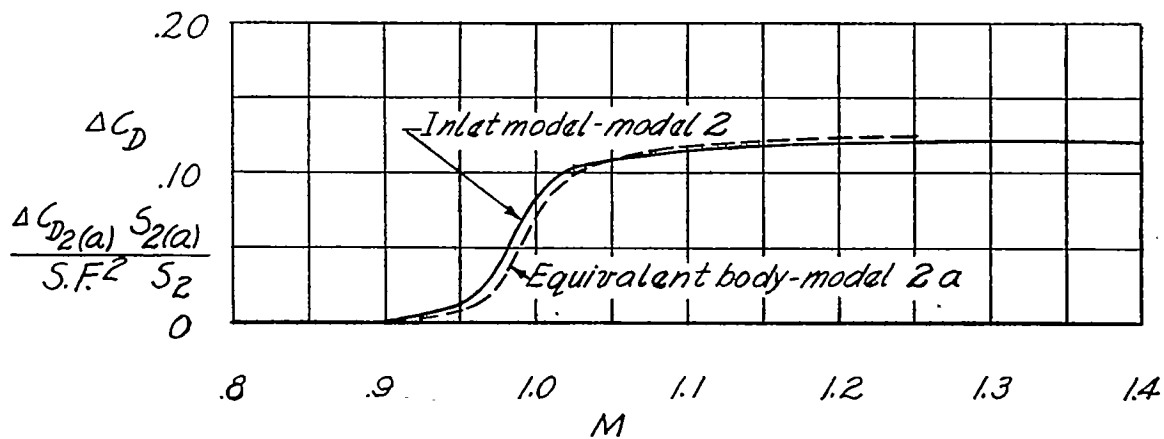


(b) Models 2 and 2(a);  $S_2 = 38.5$  sq in.;  $S_{2(a)} = 2.02$  sq in.

Figure 5.- Comparison of drag coefficients of inlet models and corresponding bodies of equivalent area distribution.



(a) Model 1 and model 1(a).



(b) Model 2 and model 2(a).

Figure 6.- Comparison of transonic drag-rise values of inlet models and bodies of equivalent area distributions.